The EMBO Journal (2011) 30, 4586–4600 | © 2011 European Molecular Biology Organization | All Rights Reserved 0261-4189/11
www.embojournal.org

THE EMBO JOURNAL

Jarid1b targets genes regulating development and is involved in neural differentiation

Sandra U Schmitz[1,2,5], Mareike Albert[1,2,5], Martina Malatesta[1,2], Lluis Morey[1,2,6], Jens V Johansen[1,3], Mads Bak[4], Niels Tommerup[4], Iratxe Abarrategui[1,2] and Kristian Helin[1,2,*]

[1]Biotech Research and Innovation Centre (BRIC), University of Copenhagen, Copenhagen, Denmark, [2]Centre for Epigenetics, University of Copenhagen, Copenhagen, Denmark, [3]The Bioinformatics Centre, Department of Biology, University of Copenhagen, Copenhagen, Denmark and [4]Wilhelm Johannsen Centre for Functional Genome Research, Department of Cellular and Molecular Medicine, University of Copenhagen, Copenhagen, Denmark

H3K4 methylation is associated with active transcription and in combination with H3K27me3 thought to keep genes regulating development in a poised state. The contribution of enzymes regulating trimethylation of lysine 4 at histone 3 (H3K4me3) levels to embryonic stem cell (ESC) self-renewal and differentiation is just starting to emerge. Here, we show that the H3K4me2/3 histone demethylase Jarid1b (Kdm5b/Plu1) is dispensable for ESC self-renewal, but essential for ESC differentiation along the neural lineage. By genome-wide location analysis, we demonstrate that Jarid1b localizes predominantly to transcription start sites of genes encoding developmental regulators, of which more than half are also bound by Polycomb group proteins. Virtually all Jarid1b target genes are associated with H3K4me3 and depletion of Jarid1b in ESCs leads to a global increase of H3K4me3 levels. During neural differentiation, Jarid1b-depleted ESCs fail to efficiently silence lineage-inappropriate genes, specifically stem and germ cell genes. Our results delineate an essential role for Jarid1b-mediated transcriptional control during ESC differentiation.

The EMBO Journal (2011) **30,** 4586–4600. doi:10.1038/emboj.2011.383; Published online 21 October 2011
Subject Categories: chromatin & transcription; development
Keywords: ES cell; histone demethylase; Jarid1b; knockout mouse; neural differentiation

Introduction

Embryonic stem cells (ESCs) have to constantly balance their potential to self-renew and differentiate (Niwa, 2007). Self-renewal and differentiation depend on the gene expression pattern in the cells, which is tightly connected with the chromatin state. Chromatin structure is influenced by post-translational histone modifications, of which a wide variety has been associated with either active transcription or gene silencing (Zhou *et al*, 2011).

Trimethylation of lysine 4 at histone 3 (H3K4me3) occurs at transcription start sites and high levels have been linked to active transcription (Schübeler *et al*, 2004; Pokholok *et al*, 2005; Barski *et al*, 2007). In concordance, a subunit of the general transcription factor TFIID can bind to this mark, which in turn may facilitate formation of the pre-initiation complex (Vermeulen *et al*, 2007). Additionally, chromatin-remodelling complexes can recognize H3K4me3 and open the chromatin structure to facilitate transcription (Wysocka *et al*, 2006; Clapier and Cairns, 2009). Yet, the association of H3K4me3 with promoters is not a definite indication for transcriptional activity (Guenther *et al*, 2007). In ESCs, the majority of promoters are H3K4me3 positive (Bernstein *et al*, 2006; Mikkelsen *et al*, 2007; Meissner *et al*, 2008); and in addition, many are marked by 'repressive' H3K27me3, a chromatin state which is referred to as bivalent (Azuara *et al*, 2006; Bernstein *et al*, 2006; Pan *et al*, 2007). In ESCs, many genes encoding developmental regulators are in this category and it has been hypothesized that bivalency is important to keep the option for all lineage choices (Azuara *et al*, 2006; Mikkelsen *et al*, 2007; Stock *et al*, 2007).

The enzyme responsible for H3K27me3 is the histone lysine methyltransferase (KMT) EZH2. EZH2 together with SUZ12 and EED forms the core of the Polycomb repressive complex 2 (PRC2), which is essential for early embryonic development (Faust *et al*, 1995; O'Carroll *et al*, 2001; Pasini *et al*, 2004). PRC2 binds to 2000–5000 genes in ESCs (Boyer *et al*, 2006; Pasini *et al*, 2007). Knockout ESCs of the distinct subunits of PRC2 all display defects in differentiation, including the neural lineage (Pasini *et al*, 2007; Shen *et al*, 2008). During differentiation the set of Polycomb group (PcG) target genes changes, indicating that PcG proteins have specific roles at given developmental states (Mohn *et al*, 2008).

A whole family of histone methyltransferases can catalyse H3K4 methylation (Hublitz *et al*, 2009; Dambacher *et al*, 2010), and like the PcG genes, several of these are important for early development and homeotic gene regulation (Yu *et al*, 1995; Yagi *et al*, 1998; Glaser *et al*, 2006). In addition, H3K4 histone methyltransferases function in haematopoiesis (Ernst *et al*, 2004) and neurogenesis (Lim *et al*, 2009). Thus, a strict regulation of H3K4 and H3K27 methylation appears to be required for normal differentiation.

Demethylation of H3K4me3 is catalysed by the Jarid1/Kdm5 family (Pedersen and Helin, 2010). There are four Jarid1 proteins in mammals, while most other species have only one homologue. The homologues in *Drosophila* (lid) and *C. elegans* (rbr-2) are important for normal development (Christensen *et al*, 2007; Li *et al*, 2008; Di Stefano *et al*, 2011). Whereas *Jarid1a* knockout mice are viable (Klose *et al*, 2007) displaying rather mild phenotypes in haematopoiesis

*Corresponding author. Biotech Research and Innovation Centre (BRIC) and Centre for Epigenetics, University of Copenhagen, Ole Maaløsvej 5, Copenhagen 2200, Denmark. Tel.: +45 3532 5666; Fax: +45 3532 5669; E-mail: kristian.helin@bric.ku.dk
[5]These authors contributed equally to this work
[6]Current address: Center for Genomic Regulation, c/ Dr Aiguader 88, 08003 Barcelona, Spain

Received: 15 May 2011; accepted: 23 September 2011; published online: 21 October 2011

 ©2011 European Molecular Biology Organization

and behaviour, it was recently reported that disruption of the *Jarid1b* locus results in early embryonic lethality (Catchpole *et al*, 2011). Moreover, high ectopic expression of Jarid1b in mouse ESCs impairs general cell specification and interferes with neural differentiation (Dey *et al*, 2008).

The role of H3K4me3 and bivalency remains important questions in stem cell biology, particularly with respect to the switch from self-renewal to differentiation. Recently, Jiang *et al* (2011) showed that decreased levels of H3K4me3 are tolerable in ESCs, but interfere with differentiation. Globally, H3K4me3 decreases during differentiation (Ang *et al*, 2011) along with the resolution of a proportion of bivalent genes to H3K27me3 only and demethylation of a subset of H3K4me3-positive promoters (Bernstein *et al*, 2006). Here, we address the role of the H3K4me2/3 demethylase Jarid1b in ESC self-renewal and differentiation.

Results

Jarid1b is dispensable for ESC self-renewal, but required for neural differentiation of ESCs

Jarid1b is predominantly expressed during embryonic development, in ESCs, and in adult testis, brain, eye, spleen and thymus (Supplementary Figure S1A and B; Madsen *et al*, 2002; Frankenberg *et al*, 2007; Dey *et al*, 2008). Since ESCs can be maintained *in vitro* as pluripotent, self-renewing cells or differentiated into many different cell types of all three germ layers (Young, 2011), they provide a good model system to study lineage choices.

To understand the function of Jarid1b for stem cell self-renewal and differentiation, we knocked down Jarid1b expression by shRNA in ESCs. The knockdown did not compromise ESC morphology, expression of the pluripotency markers Oct4 and Nanog or ESC proliferation (Figure 1B; Supplementary Figure S1C–E).

While this manuscript was in preparation, another study showed that Jarid1b is required for ESC self-renewal (Xie *et al*, 2011), and an attempt to establish *Jarid1b* mutant ESCs from *Jarid1b* mutant blastocysts was unsuccessful (Catchpole *et al*, 2011). To unambiguously determine the role of Jarid1b in ESCs, we established conditional targeted *Jarid1b* ESCs, in which *Jarid1b* exon 6 is flanked by *loxP* sites (Supplementary Figure S2). Cre-mediated deletion creates a frameshift and subsequent termination mutation. In conditional *Jarid1b*$^{F/F}$; *Rosa26::CreERT2* ESC lines *Jarid1b* could be efficiently deleted by administration of 4-hydroxy-tamoxifen (4OHT; Supplementary Figures S2C and S3C). At global levels, Jarid1b was undetectable 72 h after addition of 4OHT. Expression of other Jarid1-family members remained unchanged after Jarid1b depletion (Supplementary Figure S3B). Importantly, like in Jarid1b knockdown cells, ESC morphology and self-renewal, reflected by Oct4 and Nanog protein expression, and growth rate were unaffected by *Jarid1b* deletion (Supplementary Figure S3A, C and D). Therefore, we conclude that Jarid1b is not required for ESC self-renewal.

As a general approach to address differentiation potential, we assayed embryoid body (EB) formation in stable Jarid1b knockdown and control cells. Morphologically, there was no difference and both cell lines formed EBs of similar size. However, while control cells expressed genes from all three germ layers after 9 days of differentiation, particularly ectodermal gene expression was not properly induced in Jarid1b knockdown cells (Supplementary Figure S4). In addition, we noticed that expression of the pluripotency markers Oct4 and Nanog was not efficiently silenced in Jarid1b knockdown cells upon differentiation.

To further understand the role of Jarid1b in ectodermal differentiation, we used a protocol which allows the generation of highly homogeneous neural progenitor cells (NPCs) and subsequently terminally differentiated neurons from ESCs (Bibel *et al*, 2007). Briefly, ESCs are differentiated to EBs, dissociated and plated for neuronal differentiation (schematized in Figure 1A). Jarid1b knockdown EBs had a normal morphology, and NPCs could attach. However, cells with reduced levels of Jarid1b failed to differentiate further towards neurons and did not build a neuronal network. Instead, most Jarid1b knockdown cells detached and died (Figure 1C). Importantly, the same differentiation defect was observed using *Jarid1b* knockout ESCs (Supplementary Figure S3E). The distinct stages of neural differentiation can be followed by expression of corresponding markers genes: *Oct4 (Pou5f1)* for ESCs, *Nestin* for NPCs and β-*III-Tubulin* and *TrkB* for neurons. Oct4 was downregulated during differentiation in both Jarid1b knockdown and control cells, even though the downregulation was less efficient in the knockdown. After plating, virtually all cells stained positive for Nestin, identifying them as NPCs (Figure 1D). However, since the plating step selects for neural cells, we analysed cells from dissociated EBs (day 8) before plating for Nestin expression by flow cytometry and found that the number of Nestin-positive cells was slightly but significantly reduced after Jarid1b knockdown (Supplementary Figure S5). During further differentiation, expression of the neuronal markers β-*III-Tubulin* and *TrkB* was upregulated in control cells as seen by RT–qPCR and immunofluorescence (Figure 1D and E), while this induction was not observed in the few remaining Jarid1b knockdown cells.

Cell-cycle length and proliferation have been shown to influence cell fate in neural cells (reviewed in Salomoni and Calegari, 2010). Yet, there was no difference in proliferation of Jarid1b knockdown NPCs, as measured by BrdU incorporation (Supplementary Figure S6A and C). Neither did we find a difference in the proportion of cells in different cell-cycle phases (Supplementary Figure S6B and C), pointing to a different mechanism.

Taken together, we conclude that Jarid1b is dispensable for ESC self-renewal, but important for differentiation of ESCs towards the neural lineage. Specifically, Jarid1b seems required for efficient generation of NPCs from ESCs, and the obtained Nestin-expressing cells do not progress further in the absence of Jarid1b.

Differentiation of brain-derived conditional knockout NSCs

To further dissect at which point during differentiation Jarid1b is required, we derived *Jarid1b*$^{F/F}$; *Rosa26::CreERT2* neural stem cells (NSCs) from the cerebral cortex of E12.5 mouse embryos. Brain-derived NSCs can be differentiated *in vitro* into neurons (preferentially during early passages) and astrocytes (later passages) (Hirabayashi and Gotoh, 2010) as illustrated in Figure 2A. In conditional knockout NSCs, *Jarid1b* was efficiently depleted within 72 h after addition of 4OHT (Figure 2B). Upon withdrawal of the growth factors

©2011 European Molecular Biology Organization

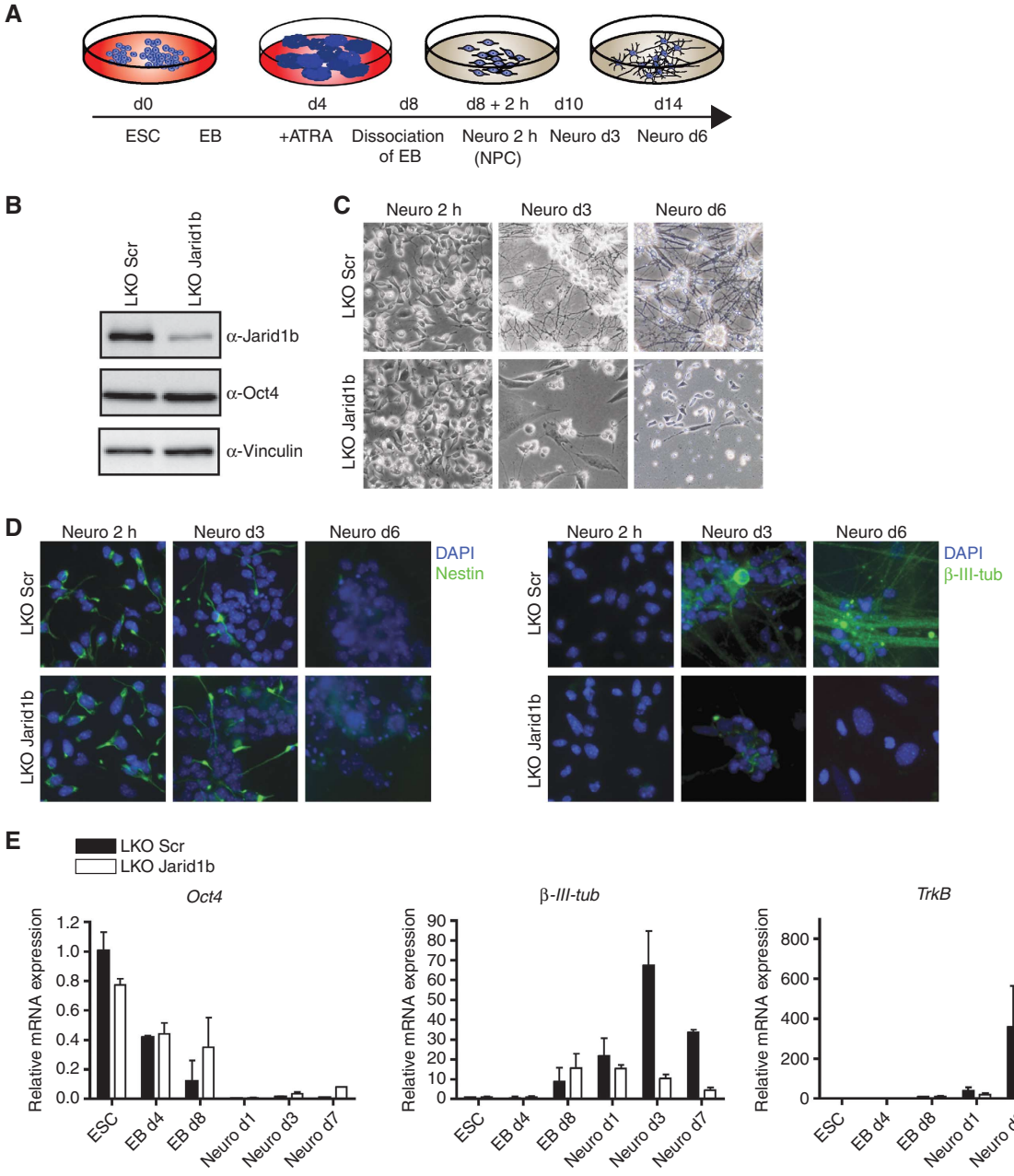

Figure 1 Neural differentiation of Jarid1b knockdown ESCs is impaired. (**A**) Schematic representation of experimental outline. ESC, embryonic stem cell; EB, embryoid body; ATRA, all-trans retinoic acid; NPC, neural precursor cell. (**B**) Immunoblots of stable lentiviral knockdown (LKO) Scramble (Scr) and Jarid1b ESC lines probed for Jarid1b, the stem cell marker Oct4 and Vinculin (loading control). (**C**) Light microscope images of Scr and Jarid1b knockdown ESCs differentiated into neural progenitor cells (NPCs, Neuro 2 h) and neurons (Neuro d3 and d6). (**D**) Immunofluorescence staining of differentiated Scr and Jarid1b knockdown ESCs for the neural stem cell marker Nestin and the neuronal marker β-III-Tubulin. DNA is stained with DAPI. (**E**) Expression of the stem cell marker *Oct4* and the neuronal marker genes β-*III-Tubulin* and *TrkB* during neural differentiation determined by quantitative RT–PCR analysis (normalized to *Rplp0* levels).

EGF/bFGF and addition of serum, both control and *Jarid1b*-deficient early passage NSCs induced expression of the neuronal genes β-*III-Tubulin* and *TrkB* and efficiently differentiated into neurons (Figure 2C and D). However, we noticed that downregulation of the NSC marker Nestin was delayed in *Jarid1b* knockout cells (Figure 2E), which is in analogy to delayed downregulation of stem cell genes during ESC differentiation. This suggests that the crucial effect of Jarid1b is established before the NSC stage and that Jarid1b is dispensable for neuronal differentiation of established NSCs.

Jarid1b occupies developmental regulators in ESCs

To understand the mechanism by which Jarid1b regulates ESC differentiation, we identified the global binding pattern of Jarid1b by chromatin immunoprecipitation (ChIP) followed by sequencing in ESCs. We generated a rabbit polyclonal antibody against a peptide corresponding to amino acids 1395–1418 of Jarid1b, a region that has very little homology to the other Jarid1-family members. The affinity-purified antibody was specific for Jarid1b as tested in western blot and ChIP in knockdown cells (Figures 1B and 3D). Deep

 ©2011 European Molecular Biology Organization

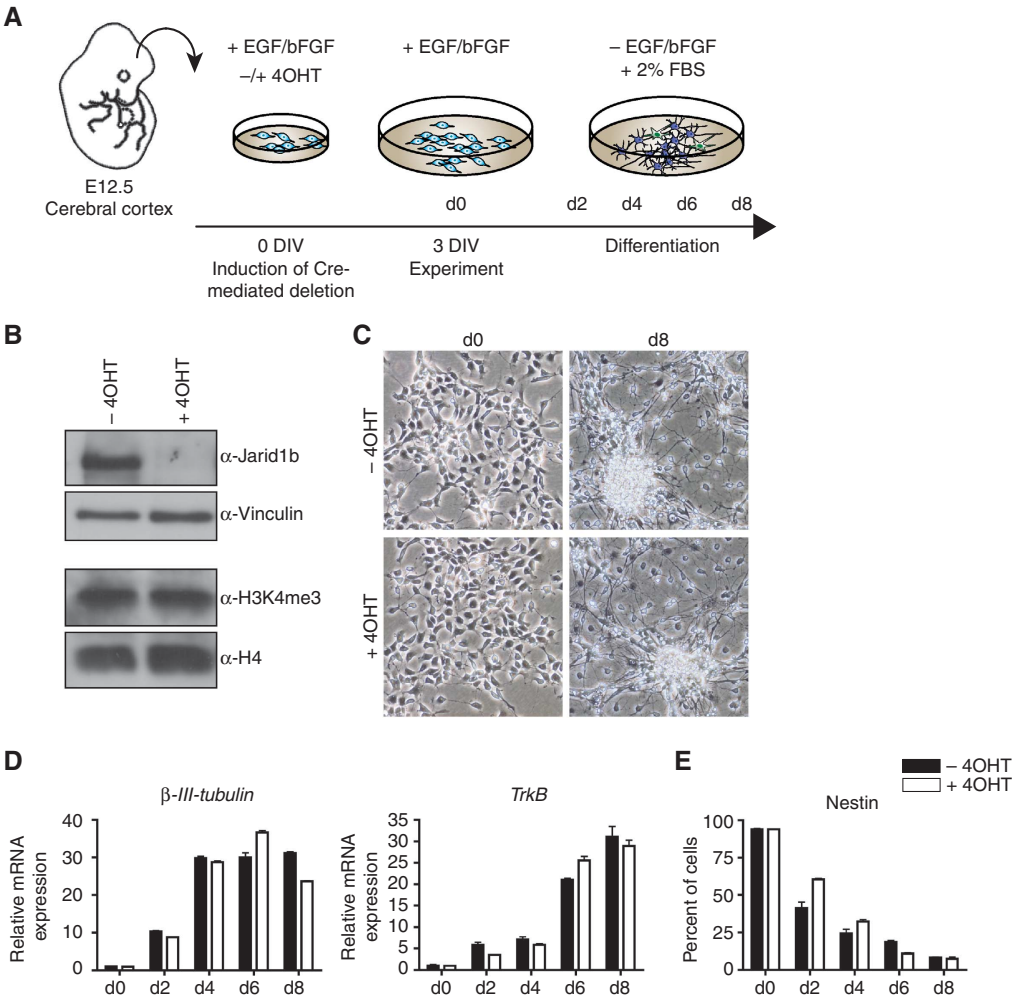

Figure 2 Jarid1b is not required for differentiation of neural stem cells derived from brain. (**A**) Schematic representation of experimental outline. DIV: days *in vitro*. (**B**) Immunoblots of conditional *Jarid1b* neural stem cells (NSCs) 72 h after induction of Cre-mediated deletion by 4OHT. (**C**) Phase-contrast images of *Jarid1b*$^{F/F}$ (−4OHT) and *Jarid1b*$^{-/-}$ (+4OHT) NSCs at 0 and 8 days of differentiation. (**D**) Expression of neuronal marker genes during differentiation of *Jarid1b*$^{F/F}$ (−4OHT) and *Jarid1b*$^{-/-}$ (+4OHT) NSCs determined by quantitative RT–PCR analysis (normalized to β-*actin* levels). (**E**) Immunofluorescence analysis of the neural stem cell marker Nestin performed on an automated screening platform.

sequencing of DNA from ESCs immunoprecipitated by the Jarid1b antibody resulted in 6.8 million reads. MACS (Zhang *et al*, 2008) predicted 5232 peaks with a false discovery rate (FDR) below 20% which overlapped 2347 unique genes. Examples of binding profiles are shown in Figure 3A. The majority of peaks were found around transcription start sites (34.8%) and within genes (32.7%) (Figure 3B and C). Few peaks (14.9%) were located in regions that were >100 kb away from any annotated gene. ChIP-qPCR validation in Jarid1b knockdown cells showed that the signal at target genes is strongly reduced (Figure 3D), demonstrating that the enrichment was specific for Jarid1b.

Recently, Jarid1b was reported to bind throughout intragenic regions and suggested to suppress aberrant intragenic transcription (Xie *et al*, 2011). Although we also detect Jarid1b binding in intragenic regions, this binding reflects individual peaks rather than spreading throughout the gene body as described by Xie *et al*. Specifically, 22.4% of the intragenic Jarid1b peaks overlap with CpG islands and another 19.4% corresponds to GC-rich regions not annotated as CpG islands (Supplementary Figure S7A and B). This is reminiscent of previous observations for PcG binding sites in ESCs which are highly enriched in CpG islands (Ku *et al*, 2008; Mohn *et al*, 2008). Moreover, a strong correlation between PRC2 binding intensity and GC richness has been reported (Mendenhall *et al*, 2010). Indeed, 94.5% of the intragenic Jarid1b peaks that overlap Suz12 binding sites (Pasini *et al*, 2010) are GC rich. In addition, a small fraction of intragenic peaks (3.5%) corresponds to alternative transcription start sites, while no specific sequence features were annotated for the remaining peaks (Supplementary Figure S7C and D). To analyse this further, we generated heat maps comparing genes with Jarid1b peaks at the TSS versus in intragenic regions with histone methylation patterns (Supplementary Figure S8). Both groups of Jarid1b peaks overlap with H3K4me3 signals and H3K27me3 marks a large fraction of Jarid1b peaks. In contrast, H3K36me3 is depleted at Jarid1b peaks at the TSS, consistent with previous genome-wide studies, and there is no specific enrichment of H3K36me3 at intragenic Jarid1b peaks.

To address the opposing findings between our study and that published by Xie *et al*, we tested the specificities of the

©2011 European Molecular Biology Organization

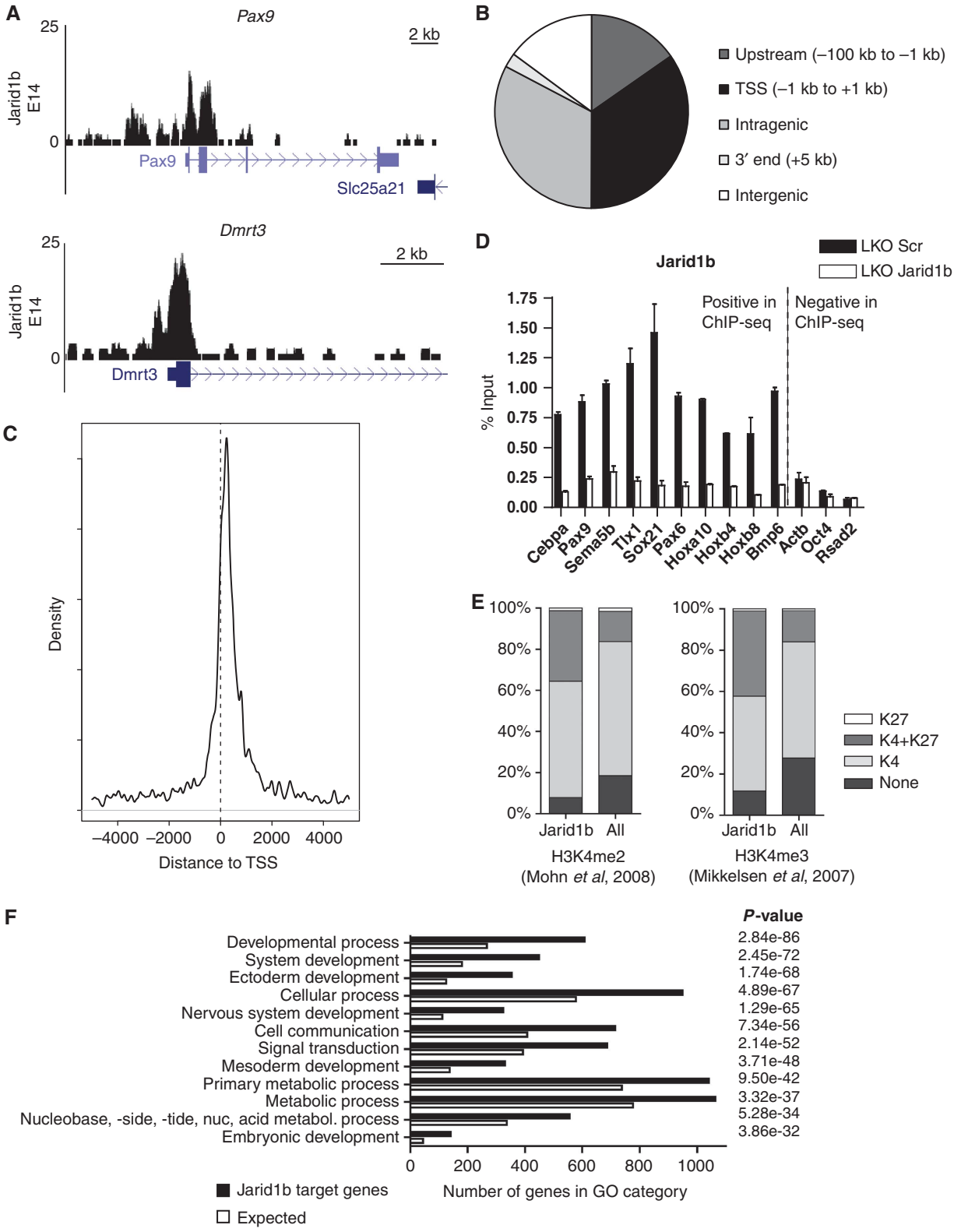

Figure 3 Jarid1b binds to transcriptional start sites of genes regulating development. (**A**) Genome-wide binding profiles of Jarid1b in E14 mouse ESCs were determined by ChIP sequencing. Two examples of binding profiles of genes bound by Jarid1b in ESCs are shown. *Y*-axis denotes number of sequence tag reads. (**B**) Distribution of Jarid1b peaks upstream of the transcriptional start site (TSS), at the TSS, in intragenic regions, at 3′ ends of genes and in intergenic regions. (**C**) Mean distribution of tags relative to the TSS (distance in bp). (**D**) ChIP-qPCR for Jarid1b of genes identified as Jarid1b positive or Jarid1b negative by ChIP-seq in LKO Scr and Jarid1b ESCs. (**E**) Percentage of H3K27me3, H3K4me2/3 (left/right panel) + H3K27me3, H3K4me2/3 (left/right panel) and unmodified promoters within Jarid1b target genes compared with all genes analysed (Mikkelsen *et al*, 2007; Mohn *et al*, 2008). (**F**) GO term analysis of genes bound by Jarid1b in ESCs. The 12 top scoring categories are presented.

©2011 European Molecular Biology Organization

antibodies used in both studies in *Jarid1b* knockout ESCs. As shown in Supplementary Figure S9, although all three antibodies confirmed loss of Jarid1b in the knockout ESCs, they showed different levels of specificity. Further, the three antibodies all led to specific enrichment of the regions reported in this manuscript. Importantly, however, only one of the antibodies used by Xie *et al* (2011) could enrich for the intragenic regions reported in their study, and this enrichment was not reduced in Jarid1b knockout cells (Supplementary Figure S9C). Based on these results, we suggest that the reported association of Jarid1b with intragenic regions (Xie *et al*, 2011) does not appear to be specific for Jarid1b.

Since H3K4me2/3 is the substrate for Jarid1b, we compared Jarid1b target genes with previously mapped H3K4me2/3-associated genes in ESCs (Mikkelsen *et al*, 2007; Mohn *et al*, 2008). To our surprise, only a very small fraction of Jarid1b target genes does not carry H3K4me2/3 (Figure 3E). In ESCs, most promoters are marked by H3K4me2/3 (Mikkelsen *et al*, 2007; Mohn *et al*, 2008); however, the proportion of H3K4me2/3-positive transcription start sites is even further enriched within the Jarid1b target gene set compared with all genes, indicating that enzyme and substrate are present at the same promoters. Moreover, the proportion of bivalent genes is notably enriched among Jarid1b target genes. In agreement with this, gene ontology analysis of Jarid1b targets identified developmental regulators including genes involved in neurogenesis and ectoderm development as significantly overrepresented (Figure 3F).

PcG proteins and Jarid1b target a similar set of genes

The finding that Jarid1b binds to bivalent regions suggests that there is an overlap between Jarid1b and PcG target genes. Indeed, we found that approximately half of the Jarid1b target genes are bound by Suz12 and in addition many are also bound by Jarid2 (Figure 4A; Pasini *et al*, 2010). Moreover, comparison with three recently defined ESC regulatory modules (Core, Polycomb and Myc) (Kim *et al*, 2010) revealed that 13.8% of Jarid1b target genes are bound by five different PcG proteins and are positive for H3K27me3, while there was no significant overlap with the Core (1.5%) or Myc (1.9%) module (Supplementary Figure S10A).

The substantial overlap between target genes raised the question if Jarid1b and PcG proteins mutually influence each other's binding. Knockdown of Jarid1b led to a small but consistent reduction of Suz12 binding at some (e.g., *Cebpa, Sema5b*) but not all genes (e.g., *Pax6*) (Figure 4B). Global protein levels of Suz12 remained unchanged (Figure 4C). The reduction of Suz12 also led to a small decrease in H3K27me3 (Figure 4B). Conversely, ChIP for Jarid1b in *Eed* knockout ESCs showed that enrichment for Jarid1b is lower in these cells than in wild-type ESCs. This effect was even more pronounced in *Ring1b* knockout ESCs (Supplementary Figure S10B). Moreover, promoter H3K4me3 levels were increased in *Ring1b* knockout cells and at a subset of tested promoters in *Eed* knockout cells, probably due to reduced Jarid1b binding. Nevertheless, we could not detect a direct physical interaction between Jarid1b and PRC2 components (Supplementary Figure S10C).

Taken together, we have shown that Jarid1b binds at transcription start sites of developmental regulators, many of which are also bound by PcG proteins. Although Jarid1b and PcG proteins affect the binding of each other to a subset of target genes, neither Jarid1b nor PcG proteins are essential for each other's recruitment.

Jarid1b regulates H3K4me3 levels in ESCs

In agreement with the described catalytic activity for Jarid1b, reduced levels of Jarid1b in ESCs lead to an increase of H3K4me3 at single promoters (Figure 4B) as well as globally (Figure 5A; Supplementary Figure S3C). To extend this observation to the whole genome, we performed ChIP sequencing for H3K4me3 in Jarid1b knockdown and control ESCs. Examples of two Jarid1b target genes are presented in Figure 5B. Jarid1b and H3K4me3 were found to colocalize at the same genomic regions around transcription start sites. The sum of H3K4me3 enrichment over gene bodies shows that there is both an increased signal at the transcription start site and within gene bodies at target genes in Jarid1b knockdown ESCs (Figure 5C), which is in line with Jarid1b peaks at transcription start sites and in intragenic regions. In total, the median number of reads for H3K4me3 increased 2.2-fold around transcription start sites at Jarid1b targets upon knockdown, while H3K4me3 levels at non-target genes were only mildly increased (1.4-fold; Supplementary Figure S11A).

Previous studies have shown that high H3K4me3 levels correlate with transcriptional activity (Lorincz and Schübeler, 2007). We wanted to know, how H3K4me3 levels at Jarid1b target promoters compare with genes categorized depending on transcriptional activity (Rahl *et al*, 2010). On average, H3K4me3 levels at Jarid1b target genes are lower than at highly active genes, and comparable to levels at non-productive promoters (Supplementary Figure S11B). Nonetheless, Jarid1b targets included all three categories (active, non-productive and inactive genes), with a modest enrichment of non-productive genes (Supplementary Figure S11C). The genome-wide analysis supports the idea that Jarid1b keeps H3K4me3 at low or intermediate levels, but does not eliminate the mark in ESCs.

Stem and germ cell-specific genes are incompletely silenced in Jarid1b knockdown NPCs

To understand how Jarid1b contributes to differentiation, we analysed gene expression in ESCs and NPCs with stable Jarid1b knockdown. We did not observe dramatic changes of expression, and in Jarid1b knockdown ESCs only 22 genes were changed >3-fold compared with control ESCs. Confirming our previous results, knockdown of Jarid1b did not affect expression of stem cell genes in ESCs. Despite the substantial global upregulation of H3K4me3 in ESCs, the majority of differentially expressed genes in ESCs were slightly downregulated (Supplementary Figure S12). Furthermore, only 3.4% of genes bound by Jarid1b were differentially expressed, suggesting that Jarid1b does not function as a strong transcriptional regulator in ESCs undergoing self-renewal and that increased levels of H3K4me3 are tolerated in growing ESCs. This is consistent with the finding that Jarid1b is not required for ESC maintenance.

In contrast to ESCs, most of the differentially expressed genes in NPCs were upregulated (Supplementary Figure S12). By categorizing these genes based on reported functions, we found that reproduction-related genes (Weber *et al*, 2007; Han *et al*, 2010; Matson *et al*, 2010; Sabour *et al*, 2011) were strikingly overrepresented within the group of genes upregulated in Jarid1b knockdown NPCs compared with control NPCs (Figure 6A). In addition, as already noticed during EB

©2011 European Molecular Biology Organization

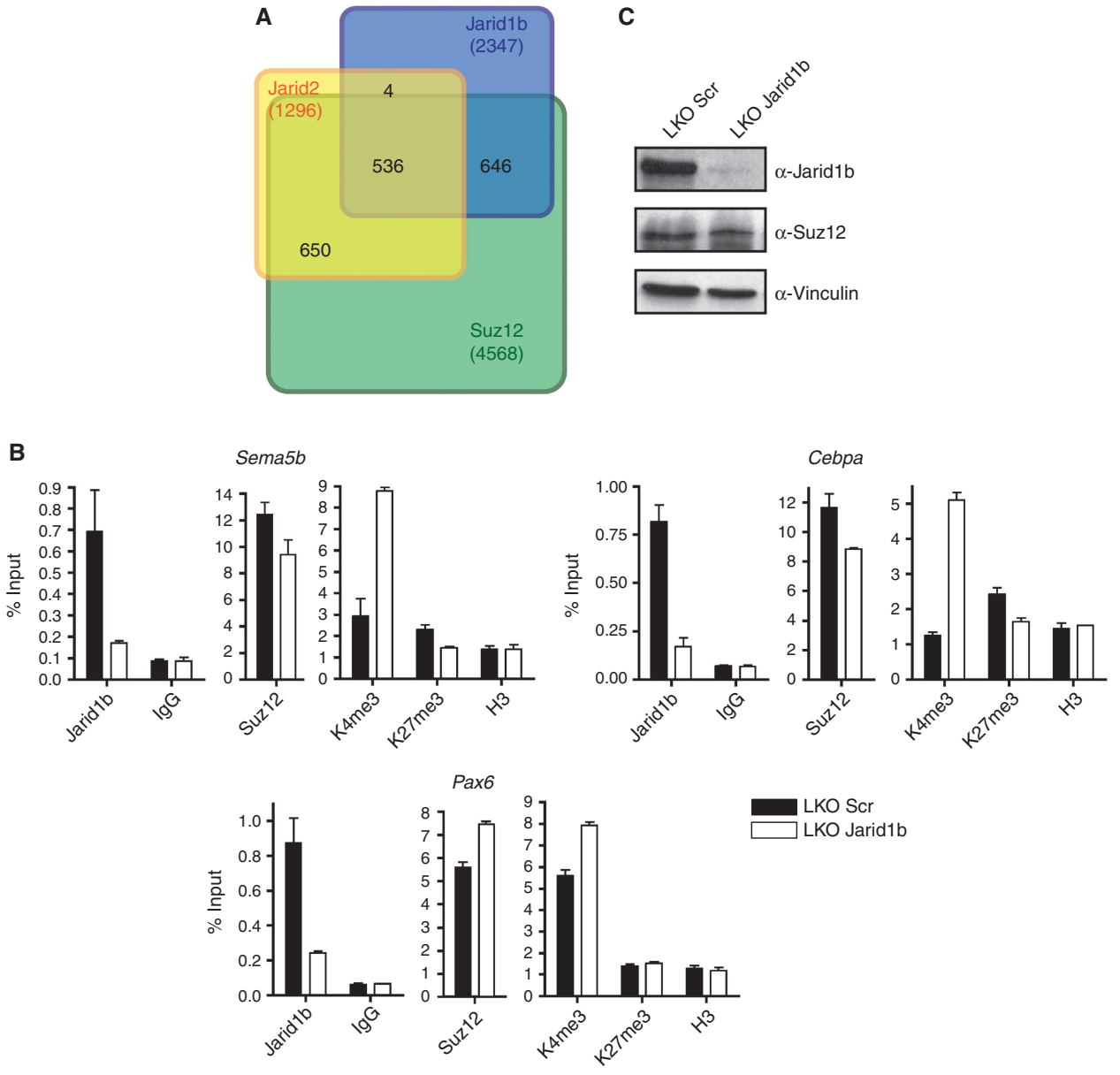

Figure 4 Polycomb proteins and Jarid1b occupy a similar set of genes in ESCs. (**A**) Venn diagram of the overlap of Jarid1b, Suz12 and Jarid2 (Pasini *et al*, 2010) target genes identified by ChIP-seq in ESCs. (**B**) ChIP-qPCR for Jarid1b, Suz12, H3K4me3, H3K27me3 and H3 in LKO Scr and Jarid1b ESCs. (**C**) Immunoblots of LKO Scr and Jarid1b ESC lines probed for Jarid1b and the polycomb protein Suz12. Vinculin was used as loading control.

differentiation (Supplementary Figure S4), we found that many pluripotency markers (Han *et al*, 2010; Kamiya *et al*, 2011) were not completely silenced in NPCs, including Nanog and Fbxo15 (Figure 6A; Supplementary Figure S13A). Moreover, we also tested the expression of markers from the three germ layers (Geijsen *et al*, 2004; West *et al*, 2006; Mikkelsen *et al*, 2007; Han *et al*, 2010; Kamiya *et al*, 2011) and defined a subset of early neural marker genes based on RNAPII recruitment from ESCs to NPCs in the same differentiation system used here (Mohn *et al*, 2008). Early neural genes are similarly expressed in Jarid1b knockdown and control NPCs, which is in agreement with our previous observation that the early neural marker Nestin is induced in Jarid1b knockdown NPCs (Figure 1D). In addition, other ectoderm, endoderm and mesoderm markers did not show differential expression in NPCs with Jarid1b knockdown compared with control (Figure 6A).

These results indicate that impaired differentiation is probably not due to failed activation of lineage-specific genes or erroneous induction of alternative lineage genes, but rather caused by failure to silence previously expressed genes, including both pluripotency and germ cell-related genes. The majority of these genes normally become silenced during differentiation in all somatic cell types (Meissner *et al*, 2008; Mohn *et al*, 2008). In most cases, downregulation is accompanied by loss of H3K4me2/3 and either gain of DNA methylation or *de novo* H3K27 methylation (Meissner *et al*, 2008; Mohn *et al*, 2008). To understand the mechanism underlying incomplete silencing of stem and germ cell genes in Jarid1b knockdown cells, we analysed the chromatin

 ©2011 European Molecular Biology Organization

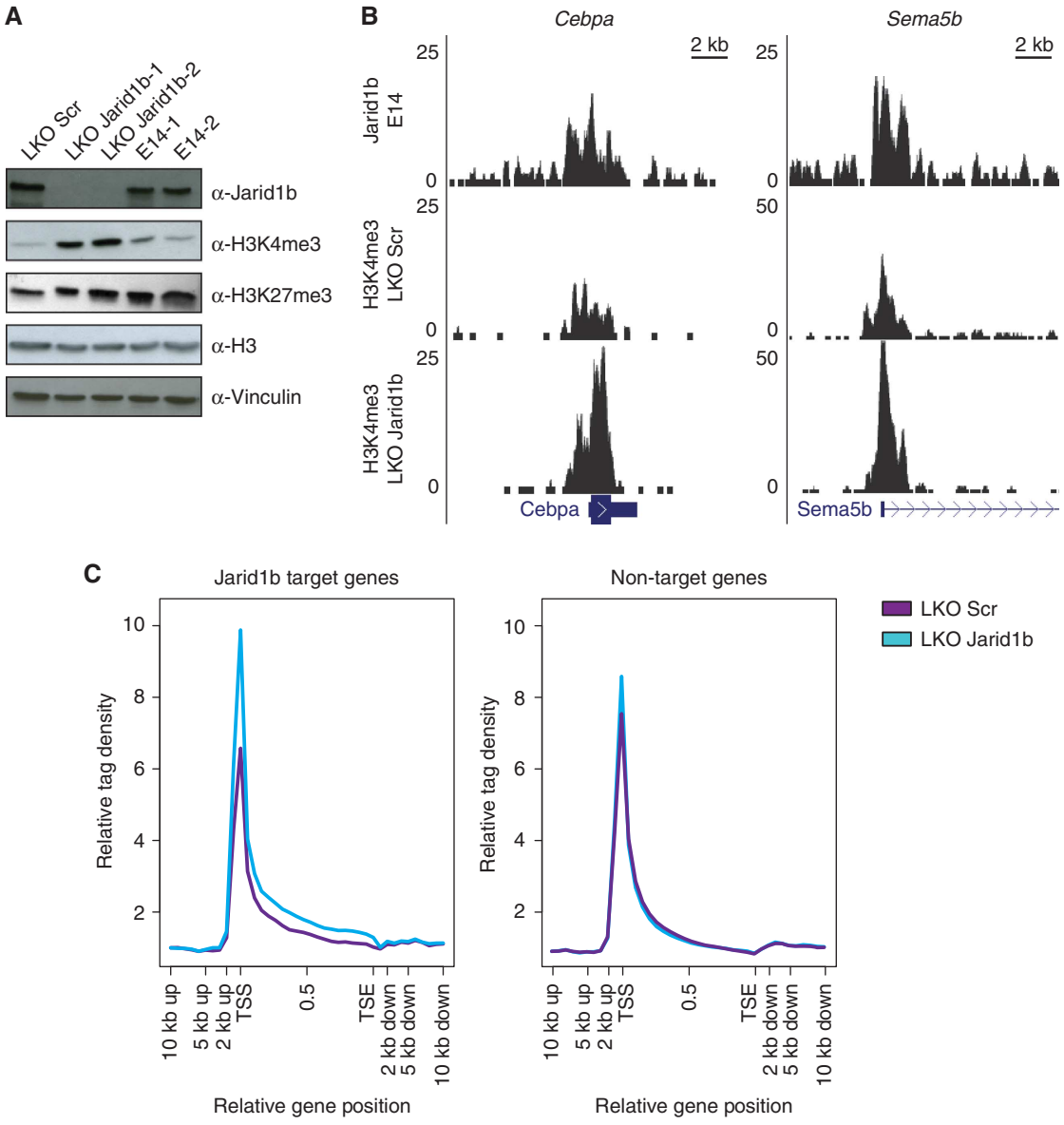

Figure 5 H3K4me3 levels are increased upon depletion of Jarid1b. (**A**) Immunoblots of LKO Scr, Jarid1b (J1b-1 and J1b-2) and control ESC lines showing increased global H3K4me3 levels in Jarid1b knockdown ESCs. H3 and Vinculin were used as loading controls. (**B**) Genome-wide profiles of H3K4me3 were determined by ChIP sequencing in LKO Scr and Jarid1b ESCs and compared with Jarid1b binding profiles. Two examples of Jarid1b target genes are presented. *Y*-axis denotes number of sequence tag reads. (**C**) Mean distribution of tags across gene bodies for H3K4me3 ChIP-seq in control and Jarid1b knockdown ESCs at Jarid1b target genes (left panel) and non-target genes (right panel).

state of *Nanog* and *Rnf17* during neural differentiation (Figure 6B). In agreement with genome-wide chromatin profiles, H3K4me3 marks both genes in ESCs. In control cells, this modification is lost during neural differentiation, while in Jarid1b knockdown NPCs both promoters retain a considerable amount of H3K4me3. This is in agreement with incomplete silencing of these genes. *Rnf17* was reported to gain DNA methylation during differentiation and to remain low for H3K27me3, while *Nanog* acquires H3K27me3 (Meissner *et al*, 2008; Mohn *et al*, 2008). Our ChIP data for H3K27me3 confirm these results, and in addition show that H3K27me3 is lower in Jarid1b knockdown NPCs. However, Jarid1b appears to be indirectly required to silence germ cell genes during neural differentiation, because we did not detect Jarid1b binding at the stem and germ cell genes tested, neither in ESCs nor in NPCs (Figure 6B and data not shown).

Discussion

Here, we have shown that Jarid1b is dispensable for ESC self-renewal, that it binds to transcription start sites of genes encoding developmental regulators, and that its inactivation leads to increased H3K4me3 levels at target promoters as well as to a global increase of H3K4me3 levels (Figure 7). Moreover, we have shown that Jarid1b is required for differentiation of ESCs along the neural lineage, which correlates with the lack of silencing of stem and germ cell genes.

Jarid1b is dispensable for ESC self-renewal

Based on siRNA/shRNA knockdown, recent publications propose that Jarid1b is a pluripotency factor required for general ESC self-renewal (Xie *et al*, 2011) and ESC proliferation (Dey *et al*, 2008). Moreover, Jarid1b mutant ESCs could not be

©2011 European Molecular Biology Organization

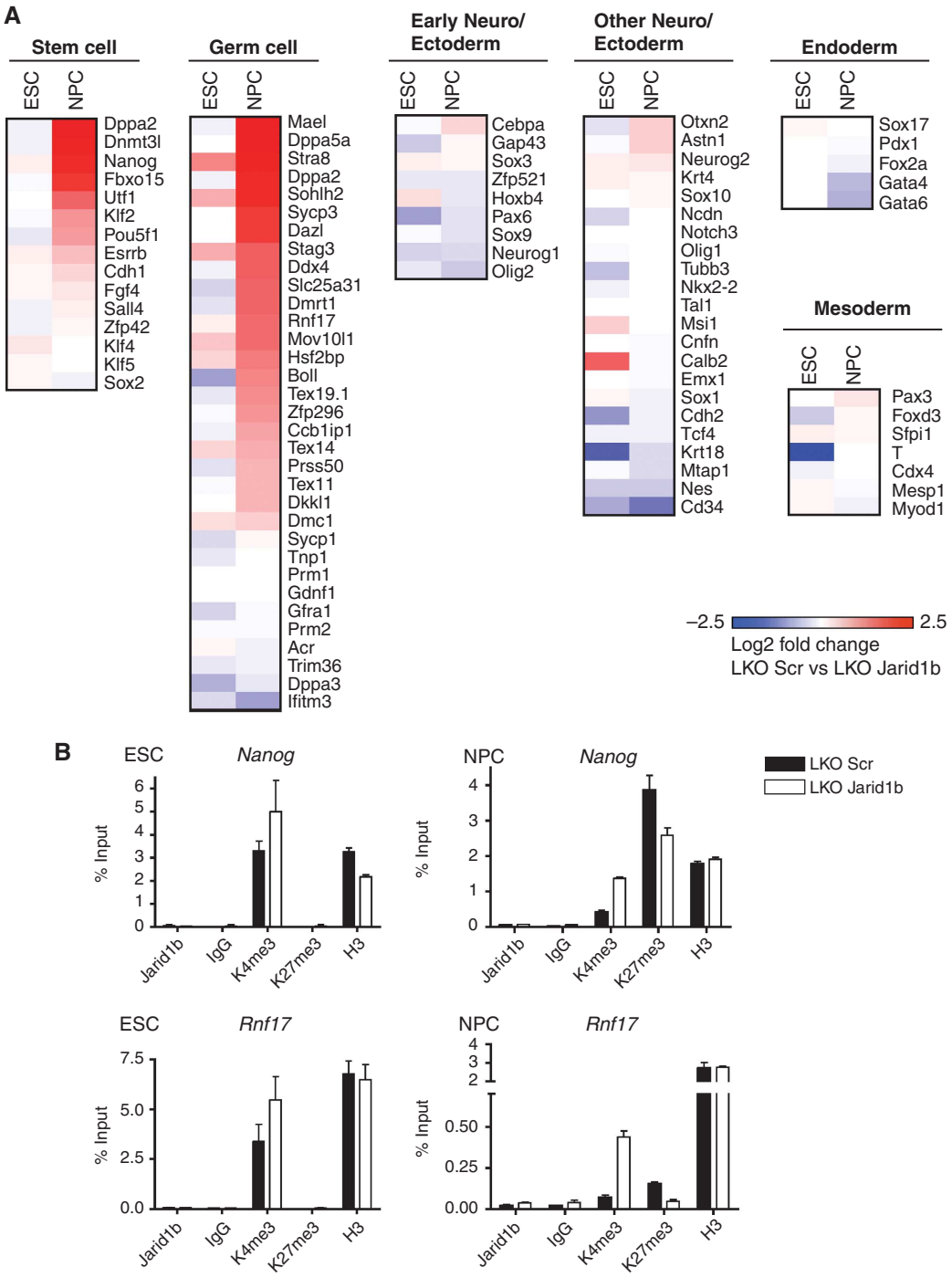

Figure 6 Incomplete downregulation of stem and germ cell genes upon differentiation of Jarid1b knockdown ESCs. (**A**) Microarray heat map depicting expression of representative self-renewal, germ cell and differentiation markers in ESCs and NPCs. Colouring illustrates log 2 fold changes between LKO Scr and Jarid1b ESCs (first column) and between LKO Scr and Jarid1b NPCs (second column) with blue and red colours representing downregulation and upregulation in knockdown, respectively. (**B**) ChIP-qPCR for Jarid1b, H3K4me3, H3K27me3 and H3 in LKO Scr and Jarid1b ESCs (left) and NPCs (right) for the stem cell gene *Nanog* and the germ cell gene *Rnf17*.

established (Catchpole *et al*, 2011). In contrast, we found that stable knockdown of Jarid1b in E14 ESCs using two different shRNA constructs does not compromise ESC proliferation or self-renewal. To exclude phenotypes due to possible shRNA off-target effects or lack of efficient downregulation of Jarid1b, we derived conditionally targeted *Jarid1b* ESCs. Importantly, complete loss of Jarid1b protein in these ESCs was confirmed using three different Jarid1b antibodies targeting both N- and C-terminal regions. In addition, transcription across the Jarid1b locus in knockout ESCs was very low (Supplementary Figure S2D), suggesting that no truncated or alternatively spliced Jarid1b protein can be produced. *Jarid1b* knockout ESCs show normal morphology, proliferation and expression of pluripotency markers both upon acute deletion and after several weeks in culture, and we therefore conclude that Jarid1b is dispensable for ESCs self-renewal.

©2011 European Molecular Biology Organization

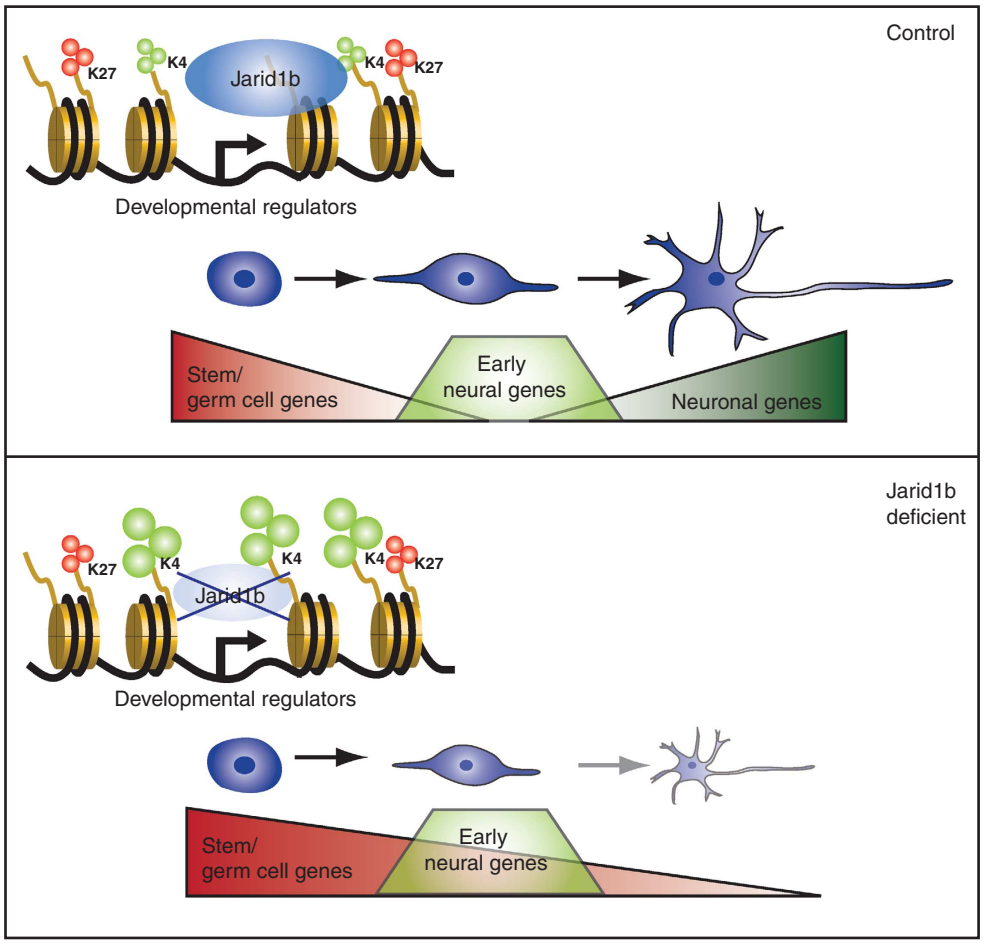

Figure 7 Model for Jarid1b function in ESCs and during neural differentiation. In mouse ESCs, Jarid1b binds to transcription start sites of genes encoding developmental regulators, of which many are marked by bivalent chromatin modifications (upper panel). Jarid1b-deficient ESCs can be maintained despite increased H3K4me3 at Jarid1b target promoters, but fail to differentiate along the neural lineage, which correlates with an inability to silence stem and germ cell-specific genes (lower panel).

Jarid1b target genes encode developmental regulators

By ChIP-seq, we found that Jarid1b binds predominantly around transcription start sites of genes encoding developmental regulators. These genes have previously been described to be marked by bivalent chromatin modifications in ESCs (Mikkelsen *et al*, 2007), and consistent with this observation, many of the Jarid1b target genes are also bound by PcG proteins and Jarid2. Jarid2 has been found to form a stable complex with PRC2 and to be essential for the binding of PcG proteins to their target genes (Peng *et al*, 2009; Shen *et al*, 2009; Pasini *et al*, 2010). In contrast, knockdown of Jarid1b only led to a small reduction of Suz12 at a subset of target promoters, indicating that Jarid1b does not recruit PcG proteins. Vice versa, Jarid1b binding is reduced, but not lost, in *Eed* and *Ring1b* knockout ESCs. Moreover, we have not detected a direct interaction between Jarid1b and PRC2, suggesting that alterations in H3K4 and H3K27 methylation might, directly or through other proteins binding to these modifications, cause the interdependent modulation of Jarid1b and PcG binding.

Our results are in contrast to a recent study that reported Jarid1b binding within intragenic regions in ESCs and that proposed a role for Jarid1b in the repression of cryptic intragenic transcription (Xie *et al*, 2011). However, we have not been able to confirm the data published by Xie *et al*, and in fact our results suggest that the enrichment of the regions published by these authors might not be specific for Jarid1b. Previously, JARID1A has also been proposed to downregulate intragenic H3K4me3 at two genes in HeLa cells, though no cryptic intragenic transcription was detected upon JARID1A deletion (Hayakawa *et al*, 2007). In contrast to these two reports (Hayakawa *et al*, 2007; Xie *et al*, 2011), Jarid1b was found to bind around transcription start sites of cancer-related genes in MCF7 cells (Yamane *et al*, 2007) and cell-cycle genes in ESCs (Dey *et al*, 2008). Likewise, Jarid1a was found to localize to promoter regions in ESCs (Pasini *et al*, 2008), MEFs (Klose *et al*, 2007) and U937 cells (Lopez-Bigas *et al*, 2008), and similarly Jarid1d occupied regions close to the transcription start site (Lee *et al*, 2007), supporting the idea that Jarid1-family members regulate gene expression through binding to transcription start sites.

Jarid1b binds to H3K4me3-positive promoters

Interestingly, the majority of Jarid1b target promoters are positive for H3K4me3, which might appear counterintuitive as Jarid1b catalyses H3K4me3 demethylation. However, the average H3K4me3 levels of Jarid1b target genes are relatively low, comparable to the levels of non-productive promoters (Rahl *et al*, 2010), suggesting that Jarid1b functions to keep H3K4me3 low rather than eliminating the mark. That is

©2011 European Molecular Biology Organization

consistent with the observation that Jarid1b binds many bivalent promoters. Likewise, JARID1A has been shown to colocalize with its substrate (Lopez-Bigas *et al*, 2008), although bivalent domains were underrepresented within JARID1A target genes in U937 cells, probably highlighting a difference to ESCs where bivalent domains are far more abundant (Mikkelsen *et al*, 2007; Mohn *et al*, 2008).

Both Jarid1a and the *Drosophila* H3K4me3 demethylase Lid harbour PHD fingers that have the potential to bind to methylated H3K4 (Wang *et al*, 2009; Li *et al*, 2010). Since two crucial residues are conserved between Jarid1a, Lid and Jarid1b (Wang *et al*, 2009), it is likely that Jarid1b also exhibits H3K4me3 affinity via one of its PHD domains, possibly contributing to its recruitment to H3K4me3-positive promoters. Supporting this idea, Jarid1b binding is reduced in ESCs with knockdown of Dpy-30 (Supplementary Figure S14), a core subunit of the SET1/MLL histone methyltransferase complexes, which regulates H3K4me3 levels in ESCs without affecting ESC self-renewal (Jiang *et al*, 2011). However, since Jarid1b is not completely lost upon Dpy-30 knockdown and moreover, does not bind to all H3K4 methylated regions, other mechanisms are likely to contribute. Jarid1b contains an Arid domain that is potentially able to directly bind DNA. Interestingly, both the Jarid1a and the Jarid1b ARID domain preferentially bind to GC-rich sequence motifs (Scibetta *et al*, 2007; Tu *et al*, 2008), and deletion of the Jarid1b ARID domain affects its histone demethylase activity (Yamane *et al*, 2007). Nonetheless, additional factors are likely to contribute specificity to cell type-dependent Jarid1b recruitment such as sequence-specific transcription factors, proteins binding to histone tails and/or specific chromatin modifications and possibly long non-coding RNAs.

Loss of Jarid1b leads to increased H3K4me3

Consistent with the previously reported catalytic activity for Jarid1b (Christensen *et al*, 2007; Yamane *et al*, 2007), H3K4me3 levels were increased at Jarid1b target genes upon Jarid1b depletion. In addition, global H3K4me3 was increased in Jarid1b knockdown and knockout ESCs. Depletion of Jarid1b in NSCs (this study) or MCF7 cells (Yamane *et al*, 2007) or depletion of Jarid1a in MEFs (Klose *et al*, 2007) did not result in a global elevation of H3K4me3 levels, suggesting that the global increase is specific to ESCs. In this respect, it is interesting to note that many promoters lose H3K4 during ESC differentiation (Mikkelsen *et al*, 2007; Meissner *et al*, 2008; Mohn *et al*, 2008) and global H3K4me3 levels decline from ESCs to differentiated cells (Ang *et al*, 2011), suggesting that this decrease might be instrumental for normal differentiation. It is worth noting that 23.5% of the genes bound by Jarid1b in ESCs lose H3K4me3 during neural differentiation to the NPC stage (Meissner *et al*, 2008).

Although tolerated, increased H3K4me3 levels in ESCs are accompanied by a number of changes in gene expression, which however do not appear sufficient to alter cell fate. Similarly, alterations in expression of differentiation and signalling genes were observed in ESCs lacking repressive H3K27me3, which however, in analogy to Jarid1b mutant ESCs, did not compromise ESC maintenance (Pasini *et al*, 2007; Shen *et al*, 2008). Moreover, ESCs lacking the PRC2 interacting protein Jarid2 (Shen *et al*, 2009; Pasini *et al*, 2010) or the PRC2 component Eed (Chamberlain *et al*, 2008) can be maintained in culture.

In addition, recent studies have addressed the effect of reduced H3K4me3 in ESCs. Both overexpression of Jarid1b (Dey *et al*, 2008) and depletion of RbBP5 or Dpy-30 (Jiang *et al*, 2011), core subunits of SET1/MLL H3K4 methyltransferase complexes, induced a number of changes in gene expression and reduced global H3K4me3 levels without affecting self-renewal of ESCs. In contrast, ESC self-renewal defects were observed upon depletion of Wdr5 (Ang *et al*, 2011), another core subunit of SET1/MLL complexes, which could in part be mediated through the loss of H3K4me3 but might also be attributed to its additional integration into histone acetylase complexes (see comment to Ang *et al*, 2011, published online).

Therefore, we conclude that perturbations in H3K4 and H3K27 methylation do not compromise the self-renewing capacity of ESCs and propose that methylation of H3K4 and H3K27 function to fine tune transcription rather than inducing cell fate conversions in ESCs.

Jarid1b is required for neural differentiation of ESCs

The effects of the lack of Jarid1b transcriptional control become more evident when ESCs are induced to differentiate. General differentiation of Jarid1b-depleted ESCs assayed by EB formation revealed deficiencies in the silencing of stem cell genes as well as the induction of marker genes representing all three germ layers, with strongest effects observed for the ectodermal lineage. Accordingly, differentiation of Jarid1b-depleted ESCs using a neural differentiation protocol was impaired and these cells did not progress beyond the NPC stage.

Using microarray analysis, we identified differentially expressed genes in NPCs most of which were upregulated, consistent with the reported role of Jarid1 proteins as transcriptional repressors (Tan *et al*, 2003; Klose *et al*, 2007). Specifically, we found that stem and germ cell-specific genes, which normally are expressed in ESCs but silenced during neural differentiation (Meissner *et al*, 2008; Mohn *et al*, 2008), are not properly switched off in Jarid1b-depleted NPCs. Thus, although NPCs expressing early neural markers could be obtained from Jarid1b mutant ESCs, the inefficient silencing of stem and germ cell genes might prevent the NPCs from further commitment towards mature neuronal cells.

Of the genes upregulated in Jarid1b knockdown NPCs, approximately half have been reported to lose H3K4me2/3 during differentiation in genome-wide chromatin-association studies (Meissner *et al*, 2008; Mohn *et al*, 2008). Loss of H3K4 methylation is a strong predictor of inverse changes in DNA methylation (Meissner *et al*, 2008), and indeed, a substantial proportion of stem and germ cell genes acquire DNA methylation from ESCs to neural cells (Meissner *et al*, 2008; Mohn *et al*, 2008). As we could not detect Jarid1b binding at stem and germ cell genes, Jarid1b seems to indirectly affect the demethylation of H3K4, which in turn may prevent CpG *de novo* methylation to occur (Ooi *et al*, 2007; Weber *et al*, 2007; Meissner *et al*, 2008). In addition, a different subset of stem and germ cell genes is silenced by *de novo* H3K27me3 (Mohn *et al*, 2008). A recent study suggests that adjustment of high H3K4me3 to moderate or low levels may modulate PcG-mediated H3K27me3 (Schmitges *et al*, 2011).

It is conceivable that, during neural differentiation, Jarid1b contributes to active demethylation of genes already bound in ESCs, possible requiring additional cues, or by being

 ©2011 European Molecular Biology Organization

recruited to new target genes. Moreover, it has been proposed that poised chromatin states in ESCs are central for the developmental potential of these cells (Pietersen and van Lohuizen, 2008). Thus, inappropriate chromatin priming in Jarid1b knockdown ESCs may interfere with the execution of differentiation programs. Due to complex interrelationships of diverse histone modifications, multiple layers of factors binding to these modifications and feedback from transcriptional activity itself, it is very difficult to dissect the contribution of each individual component in a dynamic differentiation system.

To further refine the requirement of Jarid1b for neural differentiation, we extended our study to Jarid1b knockout NSCs isolated from embryonic brain. We found that Jarid1b is not required for the generation of neurons from these NSCs. Importantly, stem and germ cell-specific genes remained undetectably low upon deletion of Jarid1b in established NSCs, suggesting that once stable silencing mechanisms like DNA methylation or H3K27me3 are in place, Jarid1b is dispensable for maintenance of the silent state. Interestingly, however, we observed a delay in the downregulation of the NSC marker Nestin during differentiation of Jarid1b knockout NSCs. This finding suggests that Jarid1b functions are cell type-specific, in analogy to cell type-specific target genes described for PcG proteins (Mohn *et al*, 2008). Nonetheless, the observed effect in NSCs is very mild, highlighting the proposed role of Jarid1b as a fine tuner of gene expression.

Jarid1b and development

Recently, it was reported that *Jarid1b* knockout mice in which exon 1 was replaced by the Neomycin gene are embryonic lethal between E4.5 and E7.5 (Catchpole *et al*, 2011) a quite severe early embryonic phenotype, also in comparison with described PcG mutants (Faust *et al*, 1995; O'Carroll *et al*, 2001; Pasini *et al*, 2004). In contrast, *Jarid1b* mutant mice established in our laboratory are viable, although at a lower Mendelian frequency, and fertile (Albert *et al*, manuscript in preparation). Thus, lack of Jarid1b seems compatible with normal gross development, possibly due to redundant functions and/or compensation by other Jarid1-family members. A detailed analysis of Jarid1b function during brain development remains to be reported, though it can be anticipated from our NSC differentiation experiments that Jarid1b might support efficient differentiation rather than being a determining factor for neuronal differentiation *in vivo*. It will be interesting to dissect Jarid1b functions in other cell types with high expression, both in normal development and in the context of cancer, where a controversial role for Jarid1b either as oncogene (Lu *et al*, 1999; Barrett *et al*, 2002; Yamane *et al*, 2007; Hayami *et al*, 2010; Roesch *et al*, 2010) or as tumour suppressor (Roesch *et al*, 2006, 2008) has been proposed.

Materials and methods

ESC culture and differentiation

E14TG2a.4 feeder-independent ESCs were cultured on 0.1% gelatin-coated tissue culture plates in standard ESC medium (Pasini *et al*, 2007). All knockdown experiments were performed using stable shRNAs. Viral transductions were performed using pLKO vectors (NM_152895.1-4880s1c1 (J1b-1), NM_152895.1-4225s1c1 (J1b-2), SHC201 (Scr) (all from Sigma), and NM_024428.2-302s1c1 (Dpy-30) (Open Biosystems)). Unless otherwise indicated differently, LKO-J1b-2 was used. ESCs were transduced with lentiviral particles for 16 h, and selected with 2 μg/μl Puromycin (Invitrogen) 48 h after transduction.

EBs were generated using the 'hanging drop' method. Drops of 1000 cells in 20 μl ESC medium with 10% FBS without LIF were placed in the lid of tissue culture dishes. Aggregates were allowed to form for 48 h, harvested and plated into bacterial dishes in the same medium. In all, 0.5 μM ATRA was added to half of the plates. Homogeneous neural cells were generated as previously described (Bibel *et al*, 2007). *Ring1b* and *Eed* knockout cells were previously described (Leeb and Wutz, 2007; Shibata *et al*, 2008).

Derivation of Jarid1b knockout ESCs

Jarid1b targeted C57BL/6N ESCs were obtained from the European Conditional Mouse Mutagenesis Program (EUCOMM). A lacZ-Neo-reporter cassette flanked by *FRT* sites was inserted between exons 5 and 6, and *Jarid1b* exon 6 was flanked by *loxP* sites. The deletion of exon 6 creates a frameshift and subsequent termination mutation. *Jarid1b* targeted ESCs were analysed by Southern blotting to confirm correct position of the targeting cassette. Analysis of metaphase spreads confirmed correct karyotype. Two targeted ESC lines, F07 and F08, were selected for injection into BALB/c blastocysts. Both lines resulted in chimeric mice.

Chimeric *Jarid1b* mice were crossed to Flp-recombinase expressing mice to obtain germline transmission and at the same time generate conditional *Jarid1b* mice lacking the reporter cassette. Conditional *Jarid1b* mice were further crossed with *Rosa26::CreERT2* mice (obtained from the Jackson Laboratory). *Jarid1b*$^{F/F}$; *Rosa26::CreERT2* ESCs were derived on feeder cells from blastocysts obtained from superovulated *Jarid1b*$^{F/+}$ females mated with *Jarid1b*$^{F/+}$; *CreERT2/CreERT2* males. The sex and karyotype were determined as described (Pasini *et al*, 2007). Deletion of Jarid1b was induced by addition of 1 nM 4OHT for at least 48 h.

For genotyping of *Jarid1b* mice and cells, 5′-CCCTGGGATTGC AGTTAAAG-3′ forward, 5′-TGGCTTCCACAATCTTCAATG-3′ reverse and 5′-TGGCTTCCACAATCTTCAATG-3′ reverse primers were used to discriminate wild-type (527 bp), floxed (609 bp) and deletion (685 bp) alleles. Mice were maintained on a C57BL/6 background. All mouse work was approved by the Danish Animal Ethical Committee ('Dyreforsøgstilsynet').

Derivation of Jarid1b knockout NSCs

NSCs were isolated from the frontal cortex of E12.5 *Jarid1b*$^{F/F}$; *Rosa26::CreERT2* embryos. Briefly, pieces of cerebral cortex were treated with trypsin-EDTA at 37°C for 20 min and mechanically dissociated by pipetting after addition of soybean trypsin inhibitor (Invitrogen). NSCs were plated on poly-D-lysine (Chemicon) and laminin (Sigma)-coated culture plates at a density of 36 000 cells/mm^2 in a 1:1 mixture of DMEM/F12 and Neurobasal medium supplemented with 10 ng/ml EGF (BioSource), 20 ng/ml bFGF (BioSource), N2, B27, Penicillin, Streptomycin, Glutamax, Non-Essential Amino Acids, Sodium-Pyruvate, β-mercaptoethanol, Heparin (Sigma), BSA (Sigma) and Hepes (all from Gibco, except where otherwise indicated). Deletion of Jarid1b was induced by addition of 1 nM 4OHT for 48 h. NSCs were induced to differentiate by removal of EGF/bFGF and addition of 2% FBS (Hyclone).

Antibodies

Jarid1b Polyclonal antibody (DAIN) was generated by immunizing rabbits with a peptide corresponding to amino acids 1395–1418 of mouse Jarid1b (NP_690855.2). The antibodies were affinity purified using Sepharose (GE Healthcare) coupled to the immunogen. Antibody specificity was confirmed by immunoblotting and IP.

Additional antibodies used in this study include anti-H3K4me3 (Cell Signaling, C42D8), anti-H3K27me3 (Cell Signaling, D18C8), anti-H3 (Abcam, 1791), anti-Suz12 (Cell Signaling, D39F6), anti-Ring1b (Richly *et al*, 2010), anti-Vinculin (Sigma, V9131), anti-Nanog (Abcam, 80892), anti-Oct4 (Abcam, 19857), mouse anti-Nestin (BD Biosciences, 611659), goat anti-Nestin (Millipore, MAB353), anti-β-III-tubulin (Sigma, T5076) and anti-BrdU (Becton Dickinson, 347580), and anti-Jarid1b (Abcam, ab50958, Santa Cruz, sc-67035).

Gene expression analysis

Total RNA was isolated using the RNAeasy Minikit (Qiagen) according to the manufacturer's instructions. cDNA was synthesized using the TaqMan Reverse Transcription kit (Applied Biosystems). qPCR was performed using SYBR Green 2× PCR Master mix (Applied Biosystems) on an ABI Prism 7300 Real-Time PCR system (Applied Biosystems) or on a LightCycler 480 System (Roche Applied Science), using the LightCycler 480 SYBR Green I

©2011 European Molecular Biology Organization

Master mix (Roche Applied Science) according to the manufacturers' instructions. Error bars represent standard deviation of three PCR amplifications for each sample. Similar results were obtained in at least three independent experiments. Primer sequences are provided in Supplementary Table I.

For microarray analysis, RNA was extracted with the RNeasy Plus kit (Qiagen). RNA was hybridized on mouse Gene 1.0 ST arrays by the RH Microarray Center at Rigshospitalet, Copenhagen, following Affymetrix procedures and analysis. Data processing and statistics were done in R using the 'affy' (RMA) and 'limma' packages. The microarray data have been submitted to the Gene Expression Omnibus (GEO) database (GSE31968). Heat maps were produced using matrix2png (Pavlidis and Noble, 2003).

ChIP assays and ChIP-seq

ChIP was performed as described (Pasini *et al*, 2010). For each IP, 0.5–1 mg of chromatin was used except for histones and histone modifications where 100 μg were used. Primer sequences are provided in Supplementary Table I.

For ChIP-seq analysis, 1 mg total protein was used. Subsequently, the DNA was adaptor-ligated, amplified using a kit from Illumina (IP-102-1001) and analysed by Solexa/Illumina high throughput sequencing. The sequence reads were aligned to the mouse genome (assembly mm9). Peak detection was performed using the MACS algorithm (Zhang *et al*, 2008) at an FDR cutoff value of <0.2. IgG was used for normalization. Chromosomal positions were annotated to the RefSeq database (mm9) using the UCSC refFlat table (Rhead *et al*, 2010). Genes not uniquely mapped to the genome were excluded. Gene overlap calculations were performed with the Galaxy browser (Giardine *et al*, 2005). Gene ontology analysis was performed using PANTHER (Thomas *et al*, 2003). GC-rich regions were defined as >100 bp long with a GC percentage of $>50\%$ and an observed/expected ratio of >0.6 (Ku *et al*, 2008). For gene body tag density, the total length of the mapped reads was extended in 3′-direction to a total length of 250 bases, which was our estimated mean fragment length after sonication. Gene bodies (defined by the longest Refseq transcript) were divided into 20 windows of equal size per gene as wells 10 windows upstream of the TSS (-10 kb) and 10 windows downstream of the TSE ($+10$ kb), for which average tag numbers were calculated. Plots showing tag density across gene bodies and peak distance to TSS were generated in R. Heat maps were generated using seqMINER (Ye *et al*, 2011). The ChIP-seq data have been submitted to the GEO database (GSE31968).

Immunofluorescence and imaging

Immunofluorescence staining was performed using standard procedures. Images were acquired on an Axioplan2 microscope (Carl Zeiss, Inc) equipped with a CoolSNAP cf2 (Photometrics) camera using MetaMorph software (MDS Analytical Technologies).

For unbiased analysis, immunofluorescence of NSC differentiation was performed in 96-well plates. Cells were imaged on an IN Cell Analyzer 1000 (GE Healthcare) utilizing a $\times 20$ objective and 10 images per well, which accounted for 1000–3000 cells. Data were analysed using IN Cell Analyzer Workstation 3.5 software (GE Healthcare). Error bars represent standard deviation of three individual wells for each sample.

Light microscope images were acquired on an Olympus IX71S8F microscope using a LOPlanFl objective.

Flow cytometry

Cells were fixed in 70% ethanol and stained with primary antibody for 1 h, followed by 1 h incubation with Alexa Fluor 488 or 647 anti-rabbit or anti-mouse IgG (Invitrogen). Cells were pulsed with 33 μM bromodeoxyuridine (BrdU) for 30 min. DNA was counterstained by 0.1 mg/ml propidium iodide supplemented with RNase for 1 h at 37°C. Analysis was performed on a FACSCalibur using CellQuest software (BD). Quantification and analysis of cell-cycle profiles were obtained using FlowJo (Tree Star, Inc).

Supplementary data

Supplementary data are available at *The EMBO Journal* Online (http://www.embojournal.org).

Acknowledgements

We thank C Steinhauer for assistance with automated image analysis and F Jia for help with mouse genotyping. We thank Anja Groth and members of the Helin laboratory for critical and fruitful discussions. MA is supported by an EMBO long-term postdoctoral fellowship. LM is supported by a CRG (Novartis) postdoctoral fellowship. The Wilhelm Johannsen Centre is supported by the Danish National Research Foundation, the Lundbeck Foundation and the Danish Ministry of Science, Technology and Innovation. Work in the Helin laboratory is supported by the Danish National Research Foundation, the Danish Cancer Society, the Novo Nordisk Foundation, the Danish Medical Research Council, the Lundbeck Foundation and the Excellence Programme of the University of Copenhagen.

Author contributions: SUS performed experiments in Figures 1, 3–6 and Supplementary Figures S1C, D, S3A, C–E, S4, S5, S8, S9C, S10–14. MA generated Figures 2, 3B, E, F and Supplementary Figures S2, S3B, S7, S10A and conditional *Jarid1b* mice and participated in analysis of ChIP sequencing and microarray experiments. MM performed experiments in Supplementary Figures S1E, S3D, S6 and S14A. LM performed experiments in Supplementary Figure S9B. JVJ provided bioinformatics support. MB and NT performed the Solexa DNA sequencing. IA developed and characterized the DAIN antibody, *Jarid1b* targeted ESCs and other reagents used in this study and performed experiments in Supplementary Figures S1A, B and S2B. SUS, MA and KH wrote the manuscript. MA and KH supervised the project.

Conflict of interest

KH is a cofounder of EpiTherapeutics and has shares and warrants in the company.

References

Ang Y-S, Tsai S-Y, Lee D-F, Monk J, Su J, Ratnakumar K, Ding J, Ge Y, Darr H, Chang B, Wang J, Rendl M, Bernstein E, Schaniel C, Lemischka IR (2011) Wdr5 mediates self-renewal and reprogramming via the embryonic stem cell core transcriptional network. *Cell* **145:** 183–197

Azuara V, Perry P, Sauer S, Spivakov M, Jørgensen HF, John RM, Gouti M, Casanova M, Warnes G, Merkenschlager M, Fisher AG (2006) Chromatin signatures of pluripotent cell lines. *Nat Cell Biol* **8:** 532–538

Barrett A, Madsen B, Copier J, Lu PJ, Cooper L, Scibetta AG, Burchell J, Taylor-Papadimitriou J (2002) PLU-1 nuclear protein, which is upregulated in breast cancer, shows restricted expression in normal human adult tissues: a new cancer/testis antigen? *Int J Cancer* **101:** 581–588

Barski A, Cuddapah S, Cui K, Roh T-Y, Schones DE, Wang Z, Wei G, Chepelev I, Zhao K (2007) High-resolution profiling of histone methylations in the human genome. *Cell* **129:** 823–837

Bernstein BE, Mikkelsen TS, Xie X, Kamal M, Huebert DJ, Cuff J, Fry B, Meissner A, Wernig M, Plath K, Jaenisch R, Wagschal A, Feil R, Schreiber SL, Lander ES (2006) A bivalent chromatin structure marks key developmental genes in embryonic stem cells. *Cell* **125:** 315–326

Bibel M, Richter J, Lacroix E, Barde Y-A (2007) Generation of a defined and uniform population of CNS progenitors and neurons from mouse embryonic stem cells. *Nat Protoc* **2:** 1034–1043

Boyer LA, Plath K, Zeitlinger J, Brambrink T, Medeiros LA, Lee TI, Levine SS, Wernig M, Tajonar A, Ray MK, Bell GW, Otte AP, Vidal M, Gifford DK, Young RA, Jaenisch R (2006) Polycomb complexes repress developmental regulators in murine embryonic stem cells. *Nature* **441:** 349–353

Catchpole S, Spencer-Dene B, Hall D, Santangelo S, Rosewell I, Guenatri M, Beatson R, Scibetta AG, Burchell JM, Taylor-Papadimitriou J (2011) PLU-1/JARID1B/KDM5B is required for embryonic survival and contributes to cell proliferation in the

 ©2011 European Molecular Biology Organization

mammary gland and in ER+ breast cancer cells. *Int J Oncol* **38:** 1267–1277

Chamberlain SJ, Yee D, Magnuson T (2008) Polycomb repressive complex 2 is dispensable for maintenance of embryonic stem cell pluripotency. *Stem Cells* **26:** 1496–1505

Christensen J, Agger K, Cloos PAC, Pasini D, Rose S, Sennels L, Rappsilber J, Hansen KH, Salcini AE, Helin K (2007) RBP2 belongs to a family of demethylases, specific for tri-and dimethylated lysine 4 on histone 3. *Cell* **128:** 1063–1076

Clapier CR, Cairns BR (2009) The biology of chromatin remodeling complexes. *Annu Rev Biochem* **78:** 273–304

Dambacher S, Hahn M, Schotta G (2010) Epigenetic regulation of development by histone lysine methylation. *Heredity* **105:** 24–37

Dey BK, Stalker L, Schnerch A, Bhatia M, Taylor-Papidimitriou J, Wynder C (2008) The histone demethylase KDM5b/JARID1b plays a role in cell fate decisions by blocking terminal differentiation. *Mol Cell Biol* **28:** 5312–5327

Di Stefano L, Walker JA, Burgio G, Corona DFV, Mulligan P, Näär AM, Dyson NJ (2011) Functional antagonism between histone H3K4 demethylases *in vivo*. *Genes Dev* **25:** 17–28

Ernst P, Fisher JK, Avery W, Wade S, Foy D, Korsmeyer SJ (2004) Definitive hematopoiesis requires the mixed-lineage leukemia gene. *Dev Cell* **6:** 437–443

Faust C, Schumacher A, Holdener B, Magnuson T (1995) The eed mutation disrupts anterior mesoderm production in mice. *Development* **121:** 273–285

Frankenberg S, Smith L, Greenfield A, Zernicka-Goetz M (2007) Novel gene expression patterns along the proximo-distal axis of the mouse embryo before gastrulation. *BMC Dev Biol* **7:** 8

Geijsen N, Horoschak M, Kim K, Gribnau J, Eggan K, Daley GQ (2004) Derivation of embryonic germ cells and male gametes from embryonic stem cells. *Nature* **427:** 148–154

Giardine B, Riemer C, Hardison RC, Burhans R, Elnitski L, Shah P, Zhang Y, Blankenberg D, Albert I, Taylor J, Miller W, Kent WJ, Nekrutenko A (2005) Galaxy: a platform for interactive large-scale genome analysis. *Genome Res* **15:** 1451–1455

Glaser S, Schaft J, Lubitz S, Vintersten K, van der Hoeven F, Tufteland KR, Aasland R, Anastassiadis K, Ang S-L, Stewart AF (2006) Multiple epigenetic maintenance factors implicated by the loss of Mll2 in mouse development. *Development* **133:** 1423–1432

Guenther MG, Levine SS, Boyer LA, Jaenisch R, Young RA (2007) A chromatin landmark and transcription initiation at most promoters in human cells. *Cell* **130:** 77–88

Han DW, Tapia N, Joo JY, Greber B, Araúzo-Bravo MJ, Bernemann C, Ko K, Wu G, Stehling M, Do JT, Schöler HR (2010) Epiblast stem cell subpopulations represent mouse embryos of distinct pregastrulation stages. *Cell* **143:** 617–627

Hayakawa T, Ohtani Y, Hayakawa N, Shinmyozu K, Saito M, Ishikawa F, Nakayama J-I (2007) RBP2 is an MRG15 complex component and down-regulates intragenic histone H3 lysine 4 methylation. *Genes Cells* **12:** 811–826

Hayami S, Yoshimatsu M, Veerakumarasivam A, Unoki M, Iwai Y, Tsunoda T, Field HI, Kelly JD, Neal DE, Yamaue H, Ponder BAJ, Nakamura Y, Hamamoto R (2010) Overexpression of the JmjC histone demethylase KDM5B in human carcinogenesis: involvement in the proliferation of cancer cells through the E2F/RB pathway. *Mol Cancer* **9:** 59

Hirabayashi Y, Gotoh Y (2010) Epigenetic control of neural precursor cell fate during development. *Nat Rev Neurosci* **11:** 377–388

Hublitz P, Albert M, Peters AHFM (2009) Mechanisms of transcriptional repression by histone lysine methylation. *Int J Dev Biol* **53:** 335–354

Jiang H, Shukla A, Wang X, Chen W-Y, Bernstein BE, Roeder RG (2011) Role for Dpy-30 in ES cell-fate specification by regulation of H3K4 methylation within bivalent domains. *Cell* **144:** 513–525

Kamiya D, Banno S, Sasai N, Ohgushi M, Inomata H, Watanabe K, Kawada M, Yakura R, Kiyonari H, Nakao K, Jakt LM, Nishikawa S-I, Sasai Y (2011) Intrinsic transition of embryonic stem-cell differentiation into neural progenitors. *Nature* **470:** 503–509

Kim J, Woo AJ, Chu J, Snow JW, Fujiwara Y, Kim CG, Cantor AB, Orkin SH (2010) A Myc network accounts for similarities between embryonic stem and cancer cell transcription programs. *Cell* **143:** 313–324

Klose RJ, Yan Q, Tothova Z, Yamane K, Erdjument-Bromage H, Tempst P, Gilliland DG, Zhang Y, Kaelin WG (2007) The retinoblastoma binding protein RBP2 is an H3K4 demethylase. *Cell* **128:** 889–900

Ku M, Koche RP, Rheinbay E, Mendenhall EM, Endoh M, Mikkelsen TS, Presser A, Nusbaum C, Xie X, Chi AS, Adli M, Kasif S, Ptaszek LM, Cowan CA, Lander ES, Koseki H, Bernstein BE (2008) Genomewide analysis of PRC1 and PRC2 occupancy identifies two classes of bivalent domains. *PLoS Genet* **4:** e1000242

Lee MG, Norman J, Shilatifard A, Shiekhattar R (2007) Physical and functional association of a trimethyl H3K4 demethylase and Ring6a/MBLR, a polycomb-like protein. *Cell* **128:** 877–887

Leeb M, Wutz A (2007) Ring1B is crucial for the regulation of developmental control genes and PRC1 proteins but not X inactivation in embryonic cells. *J Cell Biol* **178:** 219–229

Li F, Huarte M, Zaratiegui M, Vaughn MW, Shi Y, Martienssen R, Cande WZ (2008) Lid2 is required for coordinating H3K4 and H3K9 methylation of heterochromatin and euchromatin. *Cell* **135:** 272–283

Li L, Greer C, Eisenman RN, Secombe J (2010) Essential functions of the histone demethylase lid. *PLoS Genet* **6:** e1001221

Lim DA, Huang Y-C, Swigut T, Mirick AL, Garcia-Verdugo JM, Wysocka J, Ernst P, Alvarez-Buylla A (2009) Chromatin remodelling factor Mll1 is essential for neurogenesis from postnatal neural stem cells. *Nature* **458:** 529–533

Lopez-Bigas N, Kisiel TA, Dewaal DC, Holmes KB, Volkert TL, Gupta S, Love J, Murray HL, Young RA, Benevolenskaya EV (2008) Genome-wide analysis of the H3K4 histone demethylase RBP2 reveals a transcriptional program controlling differentiation. *Mol Cell* **31:** 520–530

Lorincz MC, Schübeler D (2007) RNA polymerase II: just stopping by. *Cell* **130:** 16–18

Lu PJ, Sundquist K, Baeckstrom D, Poulsom R, Hanby A, Meier-Ewert S, Jones T, Mitchell M, Pitha-Rowe P, Freemont P, Taylor-Papadimitriou J (1999) A novel gene (PLU-1) containing highly conserved putative DNA/chromatin binding motifs is specifically up-regulated in breast cancer. *J Biol Chem* **274:** 15633–15645

Madsen B, Spencer-Dene B, Poulsom R, Hall D, Lu PJ, Scott K, Shaw AT, Burchell JM, Freemont P, Taylor-Papadimitriou J (2002) Characterisation and developmental expression of mouse Plu-1, a homologue of a human nuclear protein (PLU-1) which is specifically up-regulated in breast cancer. *Mech Dev* **119**(Suppl 1)**:** S239–S246

Matson CK, Murphy MW, Griswold MD, Yoshida S, Bardwell VJ, Zarkower D (2010) The mammalian double sex homolog DMRT1 is a transcriptional gatekeeper that controls the mitosis versus meiosis decision in male germ cells. *Dev Cell* **19:** 612–624

Meissner A, Mikkelsen TS, Gu H, Wernig M, Hanna J, Sivachenko A, Zhang X, Bernstein BE, Nusbaum C, Jaffe DB, Gnirke A, Jaenisch R, Lander ES (2008) Genome-scale DNA methylation maps of pluripotent and differentiated cells. *Nature* **454:** 766–770

Mendenhall EM, Koche RP, Truong T, Zhou VW, Issac B, Chi AS, Ku M, Bernstein BE (2010) GC-rich sequence elements recruit PRC2 in mammalian ES cells. *PLoS Genet* **6:** e1001244

Mikkelsen TS, Ku M, Jaffe DB, Issac B, Lieberman E, Giannoukos G, Alvarez P, Brockman W, Kim T-K, Koche RP, Lee W, Mendenhall E, O'Donovan A, Presser A, Russ C, Xie X, Meissner A, Wernig M, Jaenisch R, Nusbaum C *et al* (2007) Genome-wide maps of chromatin state in pluripotent and lineage-committed cells. *Nature* **448:** 553–560

Mohn F, Weber M, Rebhan M, Roloff TC, Richter J, Stadler MB, Bibel M, Schübeler D (2008) Lineage-specific polycomb targets and *de novo* DNA methylation define restriction and potential of neuronal progenitors. *Mol Cell* **30:** 755–766

Niwa H (2007) How is pluripotency determined and maintained? *Development* **134:** 635–646

O'Carroll D, Erhardt S, Pagani M, Barton SC, Surani MA, Jenuwein T (2001) The polycomb-group gene Ezh2 is required for early mouse development. *Mol Cell Biol* **21:** 4330–4336

Ooi SKT, Qiu C, Bernstein E, Li K, Jia D, Yang Z, Erdjument-Bromage H, Tempst P, Lin S-P, Allis CD, Cheng X, Bestor TH (2007) DNMT3L connects unmethylated lysine 4 of histone H3 to *de novo* methylation of DNA. *Nature* **448:** 714–717

Pan G, Tian S, Nie J, Yang C, Ruotti V, Wei H, Jonsdottir GA, Stewart R, Thomson JA (2007) Whole-genome analysis of histone H3 lysine 4 and lysine 27 methylation in human embryonic stem cells. *Cell Stem Cell* **1:** 299–312

Pasini D, Bracken AP, Hansen JB, Capillo M, Helin K (2007) The polycomb group protein Suz12 is required for embryonic stem cell differentiation. *Mol Cell Biol* **27:** 3769–3779

©2011 European Molecular Biology Organization

Pasini D, Bracken AP, Jensen MR, Lazzerini Denchi E, Helin K (2004) Suz12 is essential for mouse development and for EZH2 histone methyltransferase activity. *EMBO J* **23:** 4061–4071

Pasini D, Cloos PAC, Walfridsson J, Olsson L, Bukowski J-P, Johansen JV, Bak M, Tommerup N, Rappsilber J, Helin K (2010) JARID2 regulates binding of the Polycomb repressive complex 2 to target genes in ES cells. *Nature* **464:** 306–310

Pasini D, Hansen KH, Christensen J, Agger K, Cloos PAC, Helin K (2008) Coordinated regulation of transcriptional repression by the RBP2 H3K4 demethylase and Polycomb-Repressive Complex 2. *Genes Dev* **22:** 1345–1355

Pavlidis P, Noble WS (2003) Matrix2png: a utility for visualizing matrix data. *Bioinformatics* **19:** 295–296

Pedersen MT, Helin K (2010) Histone demethylases in development and disease. *Trends Cell Biol* **20:** 662–671

Peng JC, Valouev A, Swigut T, Zhang J, Zhao Y, Sidow A, Wysocka J (2009) Jarid2/Jumonji coordinates control of PRC2 enzymatic activity and target gene occupancy in pluripotent cells. *Cell* **139:** 1290–1302

Pietersen AM, van Lohuizen M (2008) Stem cell regulation by polycomb repressors: postponing commitment. *Curr Opin Cell Biol* **20:** 201–207

Pokholok DK, Harbison CT, Levine S, Cole M, Hannett NM, Lee TI, Bell GW, Walker K, Rolfe PA, Herbolsheimer E, Zeitlinger J, Lewitter F, Gifford DK, Young RA (2005) Genome-wide map of nucleosome acetylation and methylation in yeast. *Cell* **122:** 517–527

Rahl PB, Lin CY, Seila AC, Flynn RA, McCuine S, Burge CB, Sharp PA, Young RA (2010) c-Myc regulates transcriptional pause release. *Cell* **141:** 432–445

Rhead B, Karolchik D, Kuhn RM, Hinrichs AS, Zweig AS, Fujita PA, Diekhans M, Smith KE, Rosenbloom KR, Raney BJ, Pohl A, Pheasant M, Meyer LR, Learned K, Hsu F, Hillman-Jackson J, Harte RA, Giardine B, Dreszer TR, Clawson H *et al* (2010) The UCSC Genome Browser database: update 2010. *Nucleic Acids Res* **38:** D613–D619

Richly H, Rocha-Viegas L, Ribeiro JD, Demajo S, Gundem G, Lopez-Bigas N, Nakagawa T, Rospert S, Ito T, Di Croce L (2010) Transcriptional activation of polycomb-repressed genes by ZRF1. *Nature* **468:** 1124–1128

Roesch A, Becker B, Schneider-Brachert W, Hagen I, Landthaler M, Vogt T (2006) Re-expression of the retinoblastoma-binding protein 2-homolog 1 reveals tumor-suppressive functions in highly metastatic melanoma cells. *J Invest Dermatol* **126:** 1850–1859

Roesch A, Fukunaga-Kalabis M, Schmidt EC, Zabierowski SE, Brafford PA, Vultur A, Basu D, Gimotty P, Vogt T, Herlyn M (2010) A temporarily distinct subpopulation of slow-cycling melanoma cells is required for continuous tumor growth. *Cell* **141:** 583–594

Roesch A, Mueller AM, Stempfl T, Moehle C, Landthaler M, Vogt T (2008) RBP2-H1/JARID1B is a transcriptional regulator with a tumor suppressive potential in melanoma cells. *Int J Cancer* **122:** 1047–1057

Sabour D, Araúzo-Bravo MJ, Hübner K, Ko K, Greber B, Gentile L, Stehling M, Schöler HR (2011) Identification of genes specific to mouse primordial germ cells through dynamic global gene expression. *Hum Mol Genet* **20:** 115–125

Salomoni P, Calegari F (2010) Cell cycle control of mammalian neural stem cells: putting a speed limit on G1. *Trends Cell Biol* **20:** 233–243

Schmitges FW, Prusty AB, Faty M, Stützer A, Lingaraju GM, Aiwazian J, Sack R, Hess D, Li L, Zhou S, Bunker RD, Wirth U, Bouwmeester T, Bauer A, Ly-Hartig N, Zhao K, Chan H, Gu J, Gut H, Fischle W *et al* (2011) Histone methylation by PRC2 is inhibited by active chromatin marks. *Mol Cell* **42:** 330–341

Schübeler D, MacAlpine DM, Scalzo D, Wirbelauer C, Kooperberg C, van Leeuwen F, Gottschling DE, O'Neill LP, Turner BM, Delrow J, Bell SP, Groudine M (2004) The histone modification pattern of active genes revealed through genome-wide chromatin analysis of a higher eukaryote. *Genes Dev* **18:** 1263–1271

Scibetta AG, Santangelo S, Coleman J, Hall D, Chaplin T, Copier J, Catchpole S, Burchell J, Taylor-Papadimitriou J (2007) Functional analysis of the transcription repressor PLU-1/JARID1B. *Mol Cell Biol* **27:** 7220–7235

Shen X, Kim W, Fujiwara Y, Simon MD, Liu Y, Mysliwiec MR, Yuan G-C, Lee Y, Orkin SH (2009) Jumonji modulates polycomb activity and self-renewal versus differentiation of stem cells. *Cell* **139:** 1303–1314

Shen X, Liu Y, Hsu Y-J, Fujiwara Y, Kim J, Mao X, Yuan G-C, Orkin SH (2008) EZH1 mediates methylation on histone H3 lysine 27 and complements EZH2 in maintaining stem cell identity and executing pluripotency. *Mol Cell* **32:** 491–502

Shibata S, Yokota T, Wutz A (2008) Synergy of Eed and Tsix in the repression of Xist gene and X-chromosome inactivation. *EMBO J* **27:** 1816–1826

Stock JK, Giadrossi S, Casanova M, Brookes E, Vidal M, Koseki H, Brockdorff N, Fisher AG, Pombo A (2007) Ring1-mediated ubiquitination of H2A restrains poised RNA polymerase II at bivalent genes in mouse ES cells. *Nat Cell Biol* **9:** 1428–1435

Tan K, Shaw AL, Madsen B, Jensen K, Taylor-Papadimitriou J, Freemont PS (2003) Human PLU-1 Has transcriptional repression properties and interacts with the developmental transcription factors BF-1 and PAX9. *J Biol Chem* **278:** 20507–20513

Thomas PD, Campbell MJ, Kejariwal A, Mi H, Karlak B, Daverman R, Diemer K, Muruganujan A, Narechania A (2003) PANTHER: a library of protein families and subfamilies indexed by function. *Genome Res* **13:** 2129–2141

Tu S, Teng Y-C, Yuan C, Wu Y-T, Chan M-Y, Cheng A-N, Lin P-H, Juan L-J, Tsai M-D (2008) The ARID domain of the H3K4 demethylase RBP2 binds to a DNA CCGCCC motif. *Nat Struct Mol Biol* **15:** 419–421

Vermeulen M, Mulder KW, Denissov S, Pijnappel WWMP, van Schaik FMA, Varier RA, Baltissen MPA, Stunnenberg HG, Mann M, Timmers HTM (2007) Selective anchoring of TFIID to nucleosomes by trimethylation of histone H3 lysine 4. *Cell* **131:** 58–69

Wang GG, Song J, Wang Z, Dormann HL, Casadio F, Li H, Luo J-L, Patel DJ, Allis CD (2009) Haematopoietic malignancies caused by dysregulation of a chromatin-binding PHD finger. *Nature* **459:** 847–851

Weber M, Hellmann I, Stadler MB, Ramos L, Pääbo S, Rebhan M, Schübeler D (2007) Distribution, silencing potential and evolutionary impact of promoter DNA methylation in the human genome. *Nat Genet* **39:** 457–466

West JA, Park I-H, Daley GQ, Geijsen N (2006) *In vitro* generation of germ cells from murine embryonic stem cells. *Nat Protoc* **1:** 2026–2036

Wysocka J, Swigut T, Xiao H, Milne TA, Kwon SY, Landry J, Kauer M, Tackett AJ, Chait BT, Badenhorst P, Wu C, Allis CD (2006) A PHD finger of NURF couples histone H3 lysine 4 trimethylation with chromatin remodelling. *Nature* **442:** 86–90

Xie L, Pelz C, Wang W, Bashar A, Varlamova O, Shadle S, Impey S (2011) KDM5B regulates embryonic stem cell self-renewal and represses cryptic intragenic transcription. *EMBO J* **30:** 1473–1484

Yagi H, Deguchi K, Aono A, Tani Y, Kishimoto T, Komori T (1998) Growth disturbance in fetal liver hematopoiesis of Mll-mutant mice. *Blood* **92:** 108–117

Yamane K, Tateishi K, Klose RJ, Fang J, Fabrizio LA, Erdjument-Bromage H, Taylor-Papadimitriou J, Tempst P, Zhang Y (2007) PLU-1 is an H3K4 demethylase involved in transcriptional repression and breast cancer cell proliferation. *Mol Cell* **25:** 801–812

Ye T, Krebs AR, Choukrallah M-A, Keime C, Plewniak F, Davidson I, Tora L (2011) seqMINER: an integrated ChIP-seq data interpretation platform. *Nucleic Acids Res* **39:** e35

Young RA (2011) Control of the embryonic stem cell state. *Cell* **144:** 940–954

Yu BD, Hess JL, Horning SE, Brown GA, Korsmeyer SJ (1995) Altered Hox expression and segmental identity in Mll-mutant mice. *Nature* **378:** 505–508

Zhang Y, Liu T, Meyer CA, Eeckhoute J, Johnson DS, Bernstein BE, Nusbaum C, Myers RM, Brown M, Li W, Liu XS (2008) Model-based analysis of ChIP-Seq (MACS). *Genome Biol* **9:** R137

Zhou VW, Goren A, Bernstein BE (2011) Charting histone modifications and the functional organization of mammalian genomes. *Nat Rev Genet* **12:** 7–18

 ©2011 European Molecular Biology Organization